COMPACT THIRD EDITION

The Rat Brain in Stereotaxic Coordinates

George Paxinos

School of Psychology
The University of New South Wales
Sydney 2052, Australia

Charles Watson

Department of Health and Behavioural Sciences
University of Wollongong
New South Wales 2521, Australia



Academic Press San Diego London Boston New York Sydney Tokyo Toronto

This book is printed on acid-free paper.

Copyright © 1997 by George Paxinos and Charles Watson

All Rights Reserved.
No part of this publication may be reproduced or transmitted in any form or by any means, electronic or mechanical, including photocopy, recording, or any information storage and retrieval system, without permission in writing from the publisher.

Academic Press, Inc.
525 B Street, Suite 1900, San Diego, California 92101-4495, USA
http://www.apnet.com

Academic Press Limited
24-28 Oval Road, London NW1 7DX, UK
http://www.hbuk.co.uk/ap/

International Standard Book Number: 0-12-547623-X

PRINTED IN THE UNITED STATES OF AMERICA
96 97 98 99 00 01 EB 9 8 7 6 5 4 3 2 1

We dedicate this book to Alexi Paxinos and John Irwin Johnson.

PREFACE: THIRD EDITION

We are brain cartographers, and, like our geographer colleagues, our central aim is to provide precise coordinates and accurate identification of features of interest. In this compact third edition of our atlas, we have used the proven stereotaxic reference system that we constructed for the first edition (Paxinos and Watson, 1982). This reference system is now universally recognized as the optimum grid for stereotaxic work in the rat brain. We have completely revised the identification of brain structures in order to produce an atlas that will be useful beyond the end of this century. We have also taken this opportunity to release the atlas in a compact form and to follow this with a comprehensive fourth edition (planned for 1997).

Features of the Compact Third Edition

- The most accurate stereotaxic reference system available
- Completely revised coronal drawings based on the photographs of the 76 coronal sections in the second edition of our atlas (Paxinos and Watson, 1986)
- Delineations assisted by consideration of separate sets of brain sections stained for parvalbumin, calbindin, calretinin, SMI-32, tyrosine hydroxylase, and NADPH diaphorase (Paxinos *et al.*, in press [a,b]), the rat nervous system textbook (Paxinos, 1995), the atlas of Swanson (1992), and other recent neuoranatomical literature
- Spinal cord drawings from the atlas of Molander and Grant (1995)
- Diagrams available on CD-Rom for printing at different magnifications

Reproduction of Atlas Figures in Other Publications

As authors, we are happy for our atlas figures to be reproduced in other publications, but we expect our work to be suitably acknowledged. If coordinates from the atlas are used, they should be acknowledged as in the following example: “Bregma 1.60 mm (Paxinos and Watson, 1996).”

Permission to reproduce the figures contained in the atlas can be obtained from the publisher:

Academic Press
Permissions Department
6277 Sea Harbor Drive
Orlando, FL
USA 32887
Telephone: (407) 345-3990
Fax: (407) 352-8860.

When requesting permission, please identify all the figures you wish to reproduce.

Allow four weeks for your request to be processed. We recommend that you use the nomenclature and abbreviation scheme that we developed for this book. This scheme has been developed on a systematic basis (see below) and is now widely recognized.

ACKNOWLEDGMENTS

We thank the following scientists who generously helped us with the delineation of particular areas: Ping-Yu Wang (brain stem), Laura Kus (cerebral cortex), Pascal Carrive (periaqueductal gray), George Alheid and Lennart Heimer (basal forebrain), Clifford Saper (parabrachial nucleus and medial preoptic area), Richard Simerly (hypothalamus), Glenda Halliday (ventral tegmental area), and Joel Elmquist (medial preoptic area). We also appreciate the advice we received from Richard Apps, Jan Arvidson, Detlef Bieger, Marco Celio, Philippe Ciofi, Gorm Danscher, Richard Harlan, Alan Harvey, Naoyuki Inagaki, Rober Jakab, Barbara Jones, Csaba Leranth, Janusz Lipski, Dan McIntyre, Neil McNaughton, Carl Marfurt, Juergen Mai, Kirsten Osen, Joel Price, Koh Shinoda, Gert Ter Horst, Joseph Travers, Thomas Van Groen, Jan Voogd, Mark Whitehead, Michael Wyss, Yukihiko Yasui, Laszlo Zaborszky, Justin Harris, and Liz Tancred.

We thank Stephen D. Marks and Connie Woodhead of Gold, Marks, Ring and Pepper for their advice.

We are grateful to Carl Molander and Gunnar Grant for allowing us to reproduce their spinal cord atlas.

The demanding work of conversion of our hand-drawn illustrations into their present digitized form was begun by Miaofen Shen and completed by Hong-Qin Wang and Luan Ling Zhang.

Hong-Qin Wang made thousands of corrections to the *Adobe Illustrator* files with a level of speed and accuracy that was outstanding. She also produced beautiful 20×24 inch photographs of the histochemical reference sections.

We thank Paul Halasz for his brilliant work in designing and assembling the CD-Rom version of this Atlas (Paxinos and Watson, 1986).

We thank Louis Tsalis for the design of the cover and Alan Brichta for drawing the skull diagram.

We thank Fine Science Tools Inc (Vancouver, Fax: 415-349-3729) for providing us with precision forceps used for the preparation of specimens. We thank Faulding Imagins for providing us with an Olympus Provis Research Microscope system at a reduced price.

We thank Professor Kevin McConkey, Head of the School of Psychology at the University of New South Wales, and Professor Gerard Sutton, Vice Chancellor of the University of Wollongong, for their generous support. We thank Apple Australia for

providing equipment to assist with digitizing the drawings for this atlas.

Finally, we are grateful to Lawrence Morrin for suggesting that we produce a compact edition of our atlas.

INTRODUCTION

There are many reasons why the rat is the most commonly selected subject for research in mammalian neuroscience. First, rats are the right size: neither too small for accurate stereotaxic localization of discrete brain areas nor too large for cost-effective laboratory management. Second, rats are generally hardy animals and are resistant to infections. Third, a number of inbred strains are available commercially; so, animals of consistent size can be used for stereotaxic procedures.

When the first edition of *The Rat Brain in Stereotaxic Coordinates* was published in 1982, it was the first atlas to be based on the flat-skull position. It offered a choice of bregma, lambda, or the midpoint of the interaural line as the reference point. Although the coordinates were developed from study of adult male Wistar rats with weights ranging from 270 to 310 g, the atlas can be successfully used with male or female rats, with weights ranging from 250 to 350 g (Paxinos *et al*., 1985).

The present atlas presents 78 diagrams of coronal sections of the brain, at intervals that average 0.25 mm. The sections were cut from unfixed brains that were frozen. The diagrams in this atlas were originally based on the study of Nissl- (cresyl violet) and acetylcholinesterase- (AChE) stained sections (see coronal photographic plates of Paxinos and Watson, 1986). The mapping of the sections for this compact third edition was assisted by the use of our sections showing the distribution of a number of antibody-based and enzyme-based stains (parvalbumin, calbindin, calretinin, SMI-32, tyrosine hydroxylase, and NADPH diaphorase). A comprehensive atlas based on chemical markers will be published by Academic Press (Paxinos *et al*., in press [a,b]).

Stereotaxic Surgery

In establishing the stereotaxic coordinate system for this atlas we studied sections from over 100 rats. To prepare these sections, we positioned the skull in a standard way (the flat-skull position) and marked the vertical and horizontal planes with needle tracks. We placed anesthetized rats in a Kopf small-animal stereotaxic instrument, and the incisor bar was adjusted until the heights of lambda and bregma were equal. This flat-skull position was achieved when the incisor bar was lowered 3.3 ± 0.4 mm below horizontal zero (Table 1).

Because the point of intersection of the lambdoid an d sagittal sutures is variable, we have chosen to define lambda as the midpoint of the curve of best fit along the lamb-

doid suture (see skull diagram). This redefined reference point is considerably more reliable than the true lambda (the point of intersection of the sagittal and lambdoid sutures), and it is located 0.3 ± 0.3 mm anterior to the interaural line. We defined bregma as the point of intersection of the sagittal suture with the curve of best fit along the coronal suture. When the two sides of the coronal suture meet the sagittal suture at different points, bregma usually falls midway between the two junctions. The anteroposterior position of bregma was 9.1 ± 0.3 mm anterior to the coronal plane passing through the interaural line, but for the brain represented in this atlas bregma is deemed to lie at 9.0 mm. The top of the skull at bregma and lambda was 10.0 ± 0.2 mm dorsal to the interaural zero plane.

To confirm the stereotaxic orientation of sections in the brain used for this atlas, reference needle tracks were made perpendicular to the horizontal and coronal planes. Vertical needle insertions were made at 2.0 mm intervals through the brain, except for the penetrations at 0.7 mm anterior to the interaural line, which was chosen to avoid rupture of a venous sinus. Ten such needle tracks appear on coronal plates of this atlas. Three horizontal needle insertions perpendicular to the coronal plane were made from the posterior of the brain at 1.0, 3.0, and 5.0 mm above the interaural line and approximately 1.0 mm lateral to the midline. The reference tracks from the horizontal needles appear as small holes in coronal sections.

Histology

After surgery, the animals were deeply anesthetized and decapitated, and their brains were frozen on dry ice within 3 min of decapitation. Brains were divided into two blocks at a plane 3.0 mm anterior to the interaural line prior to placement on the freezing microtome stage and were then sectioned coronally.

Frozen brains were sectioned on an American Optical Cryocut microtome at 40 µm. Sections were obtained parallel to the stereotaxic planes by adjusting the angle of cutting until the needle tracks encountered were judged to be parallel to the plane of section. Sections were taken directly from the cryotome knife on uncoated slides with the help of an anti-roll device. At each 0.5 mm interval, three sections were taken for staining with cresyl violet or for the demonstration of AChE. Staining was carried out on the same day as cutting. The two stains were used in an alternating fashion in relation to the section intervals. One of these sections at each interval was presented in the first edition of the atlas. In the second edition we interpolated an additional section between the 0.5 mm interval sections in most cases. In the present atlas, the interpolated sections commence after Fig. 11. An attempt was made to select interpolated sections close to the midpoint of the interval of the plates in the first edition of the atlas, but such sections often were not available, and the closest suitable section was selected. Because of this process of selection of interpolated sections, the regular alternation of Nissl- and AChE-stained sections was broken.

Table 1 Craniometric and stereotaxic data (means ± S.D.) for rats of different sex, strain, and weight

Subject	Mean weight (g)*	AP I – B (mm)	AP I – L (mm)	DV I – B (mm)	AP I – Acb (mm)**	AP B – ac (mm)**	AP I – 7n (mm)**	DV I – incisor bar (mm)
'Atlas'								
Wistar	290	9.1 ± 0.3	0.3 ± 0.3	10.0 ± 0.2	11.7	0.0	–1.3	–3.3 ± 0.4
Coronal								
plates	300	9.2	0.2	10.1				
Sagittal								
plates	270	8.9	0.0	10.0				
Horizontal								
plates	290	9.1	0.2	10.1				
Female								
Wistar	282	9.3 ± 0.2	0.5 ± 0.3	10.0 ± 0.1	11.6	0.1	–1.2	–3.2 ± 0.5
Hooded	290	9.4 ± 0.4	0.3 ± 0.6	9.8 ± 0.2	11.9	0.0	–1.2	–3.9 ± 0.6
Sprague	299	9.0 ± 0.2	0.7 ± 0.2	10.1 ± 0.1	11.7	0.1	–1.2	–3.9 ± 0.5
Juvenile								
Wistar	180	7.7 ± 0.4	–0.4 ± 0.3	9.9 ± 0.2	10.2	–0.1	–1.6	–2.0 ± 0.4
Mature								
Wistar	436	9.7 ± 0.3	0.6 ± 0.3	10.7 ± 0.4	12.4	–0.1	–0.8	–2.7 ± 0.3

* S.D.s. ≤ 20 g.

** S.D.s. ≤ 0.4 mm.

ac, anterior commissure; Acb, accumbens nucleus; AP, anterior-posterior; B, bregma; DV, dorsal-ventral; 7n, facial nerve; I, interaural line; L, lambda.

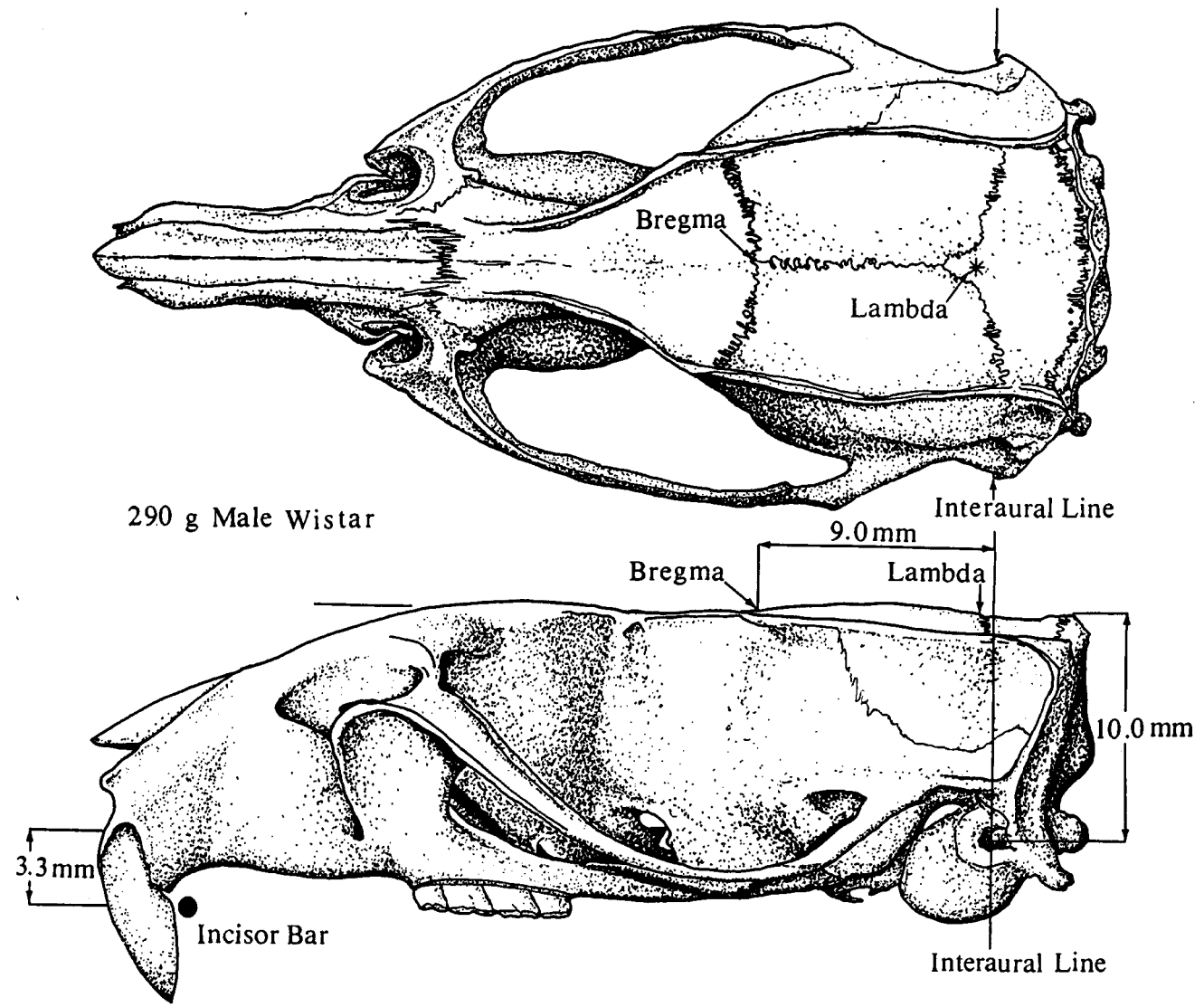
Reprinted with permission from *J. Neuroscience Methods.* **13** (1985) 139-143.

Cresyl Violet Staining

Slides were immersed for 5 min in each of the following: xylene, xylene, 100% alcohol, 100% alcohol, 95% alcohol, and 70% alcohol. They were dipped in distilled water and stained in 0.5% cresyl violet for 15-30 min. They were differentiated in water for 3-5 min and then dehydrated through 70% alcohol, 95% alcohol, 100% alcohol, and 100% alcohol. They were then put in xylene and cover-slipped. To make 500 ml of 0.5% cresyl violet of about pH 3.9, mix 2.5 g of cresylecht violet (Chroma Gesellschaft, Postfach 11 10, D-73257, Kongen, Germany, Fax number: 49-7024-82660), 300 mL of water, 30 mL of 1.0 M sodium acetate (13.6 g of granular sodium acetate in 92 mL of water), and 170 mL of 1.0 M acetic acid (29 mL of glacial acetic acid added to 471 mL of water). Mix this solution for at least 7 days on a magnetic stirrer, then filter.

AChE Histochemistry

The method for the demonstration of AChE followed the procedures of Koelle and Friedenwald (1949) and Lewis (1961). Slides were incubated for 15 h in 100 mL of stock solution (see below) to which had been added 116 mg of S-acetylthiocholine iodide and 3.0 mg ethopropazine (May & Baker). The slides were rinsed with tap water and developed for 10 min in 1% sodium sulphide (1.0 g in 100 mL of water) at pH 7.5. They were then rinsed with water and immersed in 4% paraformaldehyde in phosphate buffer for 8 h, and then allowed to dry. Subsequently, they were dehydrated for 5 min in 100% alcohol, then immersed in xylene and cover-slipped with Permount. The stock solution was a 50 mM sodium acetate buffer at pH 5.0 which was made 4.0 mM with respect to copper sulphate and 16mM with respect to glycine. This was done by adding 6.8 g of sodium acetate, 1.0 g of copper sulphate crystals, and 1.2 g of glycine to 1.0 L of water and lowering the pH to 5.0 with HCl. We found that fresh, unfixed tissue from the frozen brains showed a substantially stronger reaction for both stains than tissue fixed with formalin, paraformaldehyde, glutaraldehyde, or alcohol. A detailed protocol of the staining procedures may be obtained from George Paxinos (g.paxinos@unsw.edu.au).



Skull Diagram Dorsal and lateral views of the skull of a 290 g Wistar rat. The positions of bregma, lambda and the plane of the interaural line are shown above the lateral view. The distance between the horizontal plane passing through the interaural line is shown on the right of the lateral view. The distance between the incisor bar and the horizontal plane passing through the interaural line is shown on the left of the lateral view. Lambda (midpoint of the curve of best fit along the lambdoid suture) is 0.3 mm anterior to the coronal plane passing through the interaural line.

Photography

The drawings of the brain were traced from photographs of stained brain sections which were taken with a Nikon Multiplot macrophotographic apparatus on 4×5 inch Kodax Plus X film. High contrast (grade 4) Ilfospeed paper was used for the Nissl sections, whereas lower contrast (grade 2) paper was used for the AChE sections. Photographs of the sections (on which the present diagrams are based) can be found in the second edition of this atlas (Paxinos and Watson, 1986).

Drawings

As far as possible, we have attempted to make the drawings accurately represent the photographs. Small adjustments have been made to some sections in which the midline or cerebral cortex were distorted, but otherwise the drawings depict the asymmetries present in the sections. When part of an atlas section was missing or severely distorted, the missing part was drawn in after consideration of sections obtained from other brains.

Fiber tracts in the drawings are outlined by solid lines, and nuclei and cell groups are outlined by broken lines. In general, each abbreviation is placed in the center of the structure to which it relates; where this is not possible, the abbreviation is placed alongside the structure and a leader line is used. The abbreviations for fiber tracts and fissures are almost always positioned on the left side of the figure, and the abbreviations for nuclei and other cell groups are generally positioned on the right side. The outlines of the ventricles and aqueduct are filled in with solid black.

Stereotaxic Reference System

Two coronal and two horizontal zero-reference planes are used in these drawings; one coronal plane and one horizontal plane are related to the interaural line and the other two are related to bregma. Lambda is located 0.3 ± 0.3 mm anterior to the interaural line, and it can be used as an alternative reference point in conjunction with the dorsoventral coordinate of bregma. The position of the stereotaxic reference points and planes are indicated on the skull diagram. The stereotaxic reference grid shows 0.2 mm intervals.

In each of the coronal drawings, the large number at the bottom shows the antero-

posterior distance of the corresponding plate from the vertical plane passing through the interaural line. The large number at bottom right shows the anteroposterior distance of the plate from bregma. The small numbers on the left margin show the dorsoventral distance from the horizontal plane passing through the interaural line. The numbers on the right margin show the dorsoventral distance from the horizontal plane passing through bregma and lambda on the surface of the skull. The numbers on the top and bottom margins show the distance of structures from the midline.

An Example of Use of the Stereotaxic Reference System

In this example, we will consider the insertion of an electrode into the basolateral amygdaloid nucleus. Figure 20 shows that the center of the basolateral amygdaloid nucleus is 6.2 mm anterior to the interaural line, 1.5 mm dorsal to it, and 5.0 mm lateral to the midline. The nucleus is 2.8 mm posterior to bregma, 8.5 mm ventral to it, and 5.0 mm lateral to the midline.

Stereotaxic Accuracy

In most cases, the position of a structure is represented to an accuracy of less than 0.5 mm. Although we used medium-sized (average 290 g) male Wistar rats in the construction of this atlas, we recognize that researchers often use animals of different sex, strain, and weight. Because of this, we have estimated the error that will occur if this atlas is used with female Wistar rats, male hooded (Long Evans) rats, male Sprague Dawley rats of 290-g weight, juvenile (180 g) Wistar rats, and mature (436 g) Wistar rats. The results of these estimations are shown in Table 1 (reproduced from Paxinos *et al.*, 1985). It is evident from these studies that no substantial stereotaxic error will occur when rats of different sex and strain are chosen, provided that the rats are of similar weight to those on which the atlas is based (290 g).

Table 2 Coordinates of the bed nucleus of the anterior commissure and the trochlear nucleus obtained from the three planes

	Bed nucleus of the ant comm			Trochlear nucleus		
Plane	A-P	D-V	Lat	A-P	D-V	Lat
Coronal	8.2	3.4	0.9	1.7	3.4	0.4
Sagittal	8.0	3.4	0.9	1.8	3.5	0.4
Horizontal	8.1	3.4	0.9	1.8	3.4	0.4

For example, for rats of different sex and strain but of similar weight, the anteroposterior distance between the interaural line and bregma is between 9.0 and 9.4 mm. Similarly, the dorsoventral distance between the interaural line and the surface of the skull at bregma and lambda is very stable (9.8 – 10.1 mm). By contrast, craniometric data for juvenile (180 g) and mature (436 g) Wistar rats differ substantially from those of other groups. The anteroposterior distance between the interaural line and bregma is 7.7 mm in the juvenile and 9.7 mm in the mature rats (9.0 mm in 290-g male rats). Lambda is 0.4 mm posterior to the interaural line in the juvenile rats and 0.6 mm anterior to this line in the mature rats (0.3 mm anterior in 290-g rats). Unexpectedly, the dorsoventral distance between the interaural line and bregma for juvenile rats (9.9 mm) was almost the same as that of 290-g rats (10.0 mm). In the mature rats, the interaural line to bregma vertical distance was 10.7 mm.

In female rats, as well as in hooded, juvenile (180 g), mature (436 g) and 290-g Wistar rats, bregma was found to be above the most forward crossing fibers of the anterior commissure. This is the point at which the posterior limbs of the anterior commissure appear. These data confirm the observation of Whishaw *et al*. (1977) that bregma is more stable than the interaural line for positioning of electrodes in brain structures close to, or anterior to, bregma. However, data from insertion of needles aimed at the level where the facial nerve leaves the facial genu (Fig. 59 in this atlas) show that the interaural reference point is more stable than bregma for localization of such posterior structures. Therefore, if juvenile or mature rats are used, greater accuracy can be achieved if bregma is used as the reference point for work with rostral structures and the interaural line for work with caudal structures. A further improvement in accuracy can be obtained by taking into account the actual location of the accumbens nucleus (anterior part of Acb shown on Fig. 9) and the genu of the facial nerve (Fig. 59). In agreement with Slotnick and Brown (1980), we noticed that coordinates of structures were closer to target if the coordinates given by the interaural and bregma reference systems were averaged.

In studying the drawings of coronal sections in this atlas, it should be noted that the sections in Figs. 1–3, 40–42, and 67–76 were taken from rat brains different from the one pictured in the remaining coronal drawings. This supplementation was necessary because of distortion of the olfactory bulbs and caudal medulla in the brain from which most of the sections were taken, and because of the loss of a number of sections at the level at which the brain was blocked.

Nomenclature

There is a critical need for a stable neuroanatomical nomenclature to accurately and efficiently convey information between neuroscientists. However, many terms are still used to describe a single structure, and, in some cases, the same term is used for completely different structures. We urge you to consider the merits of our system of nomenclature because it is systematic and derived after extensive consultations with neuro-

anatomy experts.

In considering the merit of a particular term over synonyms, we have chosen terms that have been ratified by modern usage, particularly usage by experts in that field. We have used anglicized versions of terms rather than older latinized versions wherever possible, and we have in all but a handful of cases avoided the use of eponyms.

Principle of Construction of Abbreviations

Neuroscience communities concerned with different systems have developed identical abbreviations for completely different structures; for example SO stands for both supraoptic nucleus and superior olive, SC for suprachiasmatic nucleus and superior colliculus, and IC for inferior colliculus and internal capsule. In dealing with the entire nervous system (as increasingly more researchers do) these parochial abbreviation schemes become impossible to implement. An additional complication arises when homologous structures are nonetheless named or abbreviated differently in different species. We have made an effort to establish homologies and are using the same abbreviations for homologous structures in atlases of the rat (Paxinos and Watson, 1986), mouse (Franklin and Paxinos, 1996), monkey (Paxinos *et al*., in press), and human (Paxinos *et al*., 1990; Mai *et al*., in press). Atlas users may wish to reflect on the construction of the abbreviations for acetylcholinesterase (AChE) and magnesium (Mg) to get a good idea of how our list was produced. The abbreviations used in the present and in our other work were developed using the following principles:

1. The abbreviations represent the order of words as spoken in English (e.g., DLG = dorsal lateral geniculate nucleus).
2. Capital letters represent nuclei, and lower case letters represent fiber tracts. Thus, the letter "N" has not been used to denote nuclei, and the letter "t" has not been used to denote fiber tracts.
3. The general principle used in the abbreviations of the names of elements in the periodic table was followed: the capital letter representing the first letter of a word in a nucleus is followed by the lower case letter most characteristic of that word (not necessarily the second letter; e.g., Mg = magnesium; Rt = reticular thalamic nucleus).
4. Compound names of nuclei have a capital letter for each part (e.g., LPGi = lateral paragigantocellular nucleus.
5. If a word occurs in the names of a number of structures, it is usually given the same abbreviation (e.g., Rt = reticular thalamic nucleus; RtTg = reticulotegmental nucleus of the pons). Exceptions to this rule are made for well-established abbreviations such as VTA.
6. Abbreviations of brain regions are omitted where the identity of the region in question is clear from its position (CMn = centromedian thalamic nucleus; not CMnTh).
7. Arabic numerals are used instead of Roman numerals in identifying (a) cranial

nerves and nuclei (as in the Berman, 1968, atlas), and (b) layers of the spinal cord. While the spoken meaning is the same, the detection threshold is lower, ambiguity is reduced, and they are easier to position in small spaces available on diagrams.

The Basis of Delineation of Structures in This Atlas

For the third edition, we have completely reviewed our delineations of all areas of the brain. Our primary guide was an extensive collection of histochemically stained sections (monoclonal antibodies and enzyme-based stains; Paxinos *et al*, in press [a,b]). Our work has been made easier by the availability of an excellent new rat brain atlas published by Swanson (1992). We have also made extensive use of other publications from our laboratory (Paxinos, 1995; Paxinos and Huang, 1995; Paxinos *et al*., 1994) as well as of authoritative studies published in the *Journal of Comparative Neurology* and other journals. As with previous editions, we have also been assisted by the advice of many colleagues who reviewed draft illustrations (see Acknowledgments).

We present below a brief account of the basis of delineation of structures. We have not repeated here the rationale for the delineation of structures presented in the second edition (Paxinos and Watson, 1996). Readers may wish to refer to that book or consult the work of Swanson (1992) and Kruger *et al*. (1995) for the history of identification of many structures in the rat brain.

Olfactory System

Refer to Shipley *et al*. (1995) for a general description of the olfactory system. We based our delineations in part on the work of de Olmos *et al*. (1978).

The existence of the semilunar nucleus was established on the basis of NADPH-diaphorase histochemistry (Paxinos *et al*., in press [a]). We acknowledge assistance of R. Harlan and P.-Y. Wang in the identification of this structure (Ahima and Harlan, 1990; Wang and Zhang, 1995).

Basal Ganglia and Basal Forebrain

Refer to Heimer *et al*. (1995) and Fallon and Loughlin (1995) for a general description of the basal ganglia and to Alheid *et al*. (1995) for a discussion of the substantia innominata and extended amygdala.

Immunoreactivity for parvalbumin and the neurofilament protein SMI-32 identifies the ventral pallidum (Paxinos *et al*., in press [a]). We retained the term *substantia innominata* and identified dorsal, ventral (as in Grove, 1988), and basal components with the assistance of G. Alheid. The basal component is marked by some positivity in tyrosine hydroxylase but is negative for SMI-32 (although surrounding areas are positive).

The area previously called fundus striati resembles the striatum proper in some

respects and the accumbens shell in others. Given that the use of the term *fundus striati* creates problems with primate homologues, we followed the advice of G. Alheid and called it the lateral accumbens shell. The remaining accumbens is delineated in accordance with Zaborszky *et al*. (1985) and Heimer *et al*. (1991).

We followed Alheid *et al*. (1995) in the identification of the interstitial nucleus of the posterior limb of the anterior commissure (IPAC).

The reticular part of the substantia nigra can be divided into a ventrolateral and a dorsomedial component on the basis of parvalbumin and calbindin distribution (Paxinos *et al*., in press [b]). The remainder of the substantia nigra and the ventral tegmental area were delineated according to the work of McRitchie *et al*. (1996).

Septum, Hypothalamus, and Neurosecretory Nuclei

Refer to Simerly (1995), Armstrong (1995), Jakab and Leranth (1995), and Oldfield and McKinley (1995) for a general description of these structures.

In our atlas of chemical markers (Paxinos *et al*., in press [a]) we found no evidence for the existence of the septohypothalamic nucleus, and for this reason we deleted it from our drawings, allocating its supracommissural part to the ventral part of the lateral septum and its subcommissural part to the anterodorsal preoptic nucleus.

Jutting ventrolaterally from the anterodorsal preoptic nucleus is a strip which is negative for parvalbumin which we have called the *alar nucleus*. The alar nucleus displays substance P positive cell bodies but little reactivity in its neuropil (Larsen, 1992).

In the preoptic area we followed Simerly (1995) and Simerly *et al*. (1984) except for the identification of the ventromedial and ventrolateral preoptic nuclei, for which we followed Elmquist *et al*. (1996) and Sherin *et al*. (1996).

The compact part of the medial preoptic nucleus is negative for substance P (see Fig. 7 of Halliday *et al*., 1995, in which this structure is visible but not labeled).

In the lateral hypothalamus we identified a ventrolateral hypothalamus nucleus on the basis of NADPH-diaphorase reactivity (Paxinos *et al*., in press [a]). This nucleus is caudal to the ventrolateral preoptic nucleus and is found dorsal to the supraoptic nucleus.

The ventral part of dorsomedial nucleus is marked by densely stained cell bodies and terminals in NADPH-diaphorase preparations (Paxinos *et al*., in press [a]).

The gemini nucleus is a conspicuous nest of a NADPH-diaphorase cell bodies (Paxinos *et al*., in press [a]).

The parasubthalamic nucleus is present in the rat (Wang and Zhang, 1995), but it is not as impressive as the homologous structure seen in the mouse brain (Franklin and Paxinos, 1996).

The arcuate nucleus was delineated according to the work of Magoul *et al*. (1994).

See Paxinos and Watson (1986) for the identification of the striohypothalamic, magnocellular lateral hypothalamic, terete, and subincertal nuclei.

Amygdala and Bed Nucleus of Stria Terminalis

Refer to Alheid *et al*. (1995) for a general description of the amygdala and the bed nucleus of the stria terminalis.

The anterodorsal part of the medial nucleus of the amygdala and the basomedial nucleus are defined by the presence of intense NADPH-diaphorase reactivity (Paxinos *et al*., in press [a]). The lateral part of the central nucleus of the amygdala is marked by the presence of tyrosine hydroxylase fibers and AChE negativity (Paxinos *et al*., in press [a]).

Thalamus

Refer to Price (1995) for a general description of thalamic nuclei.

See Paxinos and Watson (1986) for the identification of the ethmoid, retroethmoid, subgeniculate, and precommissural nuclei.

We have reverted to the use of the term ventral posterior nucleus, parvicellular part (Paxinos and Watson, 1982) for the nucleus that we previously named the gustatory nucleus of the thalamus (Paxinos and Watson, 1986). We made this change on the advice of C. Saper that gustatory input is more medial in this nucleus, and autonomic-related inputs can be found at more lateral parts of this structure (Yasui *et al*., 1989).

Hippocampal Region

Refer to Amaral and Witter (1995) for a general description of the hippocampal region.

The postsubicular area was identified on the basis of the work of Van Groen *et al*. (1992).

Cortex

There have been two comprehensive cortical parcellation schemes in recent decades. The first one was presented by Zilles (1985) and was constructed on the original stained sections of the present atlas (updated by Zilles and Wree, 1995). In the previous edition of our atlas we used the cortical parcellations of Zilles (1985). The second comprehensive cortical delineation scheme was presented by Swanson (1992). The Zilles (1985) and Zilles and Wree (1995) works differ significantly from the Swanson (1992) scheme.

The atlas of chemical markers (Paxinos *et al*., in press [a,b]) enabled us to make a decision on the strengths of the two schemes. On this basis we have retained many of the features of the sensory, motor, and insular areas proposed by Zilles (1985). However, we have curtailed the rostral spread of Zilles's occipital areas and delineated the sensory representation of the trunk region and parietal association area in line with Swanson (1992). We have retained the perirhinal cortex at caudal levels (along with Zilles, 1985) because there is a characteristic NADPH-diaphorase reactivity associated

with this area. However, we have delineated the ectorhinal cortex and temporal association area in accordance with Swanson (1992).

Strong parvalbumin immunoreactivity is present in layer 4 of the primary somatosensory cortex. SMI-32 immunoreactivity formed distinctive patches in layer 4 of the barrel field and forelimb and hindlimb regions. The primary auditory area was identified on the basis of reduced calbindin immunoreactivity in the deep layers. All the auditory areas were marked by the presence of SMI-32 positive cells in the superficial layers. AChE marked the location of the prelimbic and agranular insular cortices. NADPH-diaphorase assisted in defining the agranular insular, perirhinal, and retrosplenial granular cortices. Additionally, NADPH-diaphorase immunoreactivity indicated the ventral part of the medial entorhinal cortex. Calretinin immunoreactivity assisted in delineation of the lateral entorhinal cortex where the outer part of layer one is densely stained.

The dorsolateral orbital cortex was delineated in accordance with the work of Ray and Price (1992).

The retrosplenial agranular cortex was delineated according to the work of Van Groen and Wyss (1992).

On the advice of Laura Kus we introduced the term *frontal association cortex* for the frontal cortex that others allocated to the secondary motor cortex (Swanson, 1992; Zilles, 1985). This designation is in agreement with microstimulation data (Neafsey *et al*., 1986).

Reticular Formation

Refer to Jones (1995) for a general description of the reticular formation.

The intermediate reticular zone was first identified in the rat (Paxinos and Watson, 1986), but is seen to advantage in the human brain (Paxinos and Huang, 1995). The intermediate reticular zone at levels of the caudal pole of the facial nerve nucleus is marked by NADPH-diaphorase positive cells.

The lateral paragigantocellular nucleus is conspicuous in NADPH-diaphorase preparations (Paxinos *et al*., in press [b]).

We have identified the parapyramidal nucleus as the cell group dorsolateral to the pyramidal tract, which is outlined but not named in the second edition of this atlas (Paxinos and Watson, 1986).

The identification of the epifascicular nucleus is based on the description of this nucleus in the human brain (Paxinos and Huang, 1995).

Periaqueductal Gray

Refer to Beitz (1995) for a general description of the periaqueductal gray. The boundaries of periaqueductal gray cell columns were drawn according to Carrive (1993), Carrive and Paxinos (1994), and Paxinos and Huang (1995).

Two nuclei lateral to the central gray pars alpha were identified on the basis of SMI-

32 immunoreactivity; P.-Y. Wang identified these structures and named them central gray pars beta and central gray pars gamma (Paxinos *et al*., in press [b]).

Tegmental Nuclei

For the identification of the anterior tegmental, microcellular tegmental, subpeducular tegmental, rabdoid, and epirubrospinal nuclei, see Paxinos and Watson (1986).

Raphe Nuclei

We identified the raphe nuclei on the basis of 5-hydroxytryptamine sections prepared by G. Halliday and I. Tork (see also Halliday *et al*., 1995). We identified the raphe interpositus nucleus on the basis of the work of Buttner-Ennever *et al*. (1988).

Locus Coeruleus and Brainstem Catecholamine Cell Groups

Refer to Aston-Jones *et al*. (1995) for the delineation of the locus coeruleus. We delineated the catecholamine cell groups by following Hokfelt *et al*. (1984) with assistance from our own tyrosine hydroxylase preparations (Paxinos *et al*., in press [b]).

Brainstem Nuclei Associated with the Respiratory Cardiovascular and Other Autonomic Functions

Refer to Saper (1995) and Norgren (1995) for a general description of these nuclei.

Nucleus of the solitary tract: The posterior part of the nucleus of the solitary tract was delineated in accordance with the work of Whitehead (1990), Herbert *et al*. (1990), McRitchie (1992), and Altschuler *et al*. (1989).

The rostral part of the nucleus of the solitary tract was difficult to delineate, but we recognize a rostrolateral subnucleus on the basis of NADPH-diaphorase positivity.

Ventral respiratory groups and Bötzinger complex: These areas were delineated in accordance with Ellenberger *et al*. (1990), Kanjhan *et al*. (1995), and Cox and Halliday (1993).

Parabrachial nucleus: The parabrachial nucleus is delineated in accordance with Fulwiler and Saper (1984), Herbert *et al.* (1990), Whitehead (1990), and Herbert and Saper (1990). The external part of the lateral parabrachial nucleus and medial parabrachial nucleus are marked by NADPH-diaphorase positive cells and fibers (Paxinos *et al*., in press [b]).

Oromotor Nuclei

Refer to Travers (1995) for a description of the oromotor nuclei.

Precerebellar Nuclei and Red Nucleus

Refer to Ruigrok and Cella (1995) for a general description of these structures. Within what has been previously called the pararubral area (Ruigrok and Cella, 1995) there is a circumscribed cell group which we called the pararubral nucleus. We have named the large cells below the minimus nucleus and above the lateral lemniscus the *epilemniscal nucleus* (Paxinos *et al*., in press [b]).

Cerebellum

The identification of lobules, fissures, and deep cerebellar nuclei is based on the work of Voogd (1995).

Somatosensory System

Refer to Tracey and Waite (1995) and Waite and Tracey (1995) for a general description of the somatosensory system. The general basis of delineation of these structures is described in Paxinos and Watson (1996). However, we followed Marfurt and Rajchert (1991) for the borders of the spinal trigeminal nucleus.

Visual System

Refer to Sefton and Dreher (1995) for a general description of the visual system.

The ventral tegmental visual relay zone was identified on the basis of the work of Giolli *et al*. (1985).

The intergeniculate leaf was delineated on the basis of the work of Morin and Blanchard (1995).

Auditory System

Refer to Webster (1995) for a general description of the auditory system. We used Faye-Lund and Osen (1985) as well as Malmierca *et al*. (1995) for the identification of areas of the inferior colliculus. The medial geniculate was delineated according to the work of LeDoux *et al*. (1985). For additional details on the basis of delineation of the components of the auditory system refer to Paxinos and Watson (1986).

References

Ahima, R. S., and Harlan, R. E. (1990). Charting of Type II glucocorticoid receptor-like immunoreactivity in the rat central nervous system. *Neuroscience* **39**, 579–604..

Alheid, G. F., de Olmos, J. S., and Beltramino, C. A. (1995). Amygdala and extended amygdala. In G. Paxinos (Ed.), The Rat Nervous System, 2nd ed. Academic Press, San Diego, pp. 495–578. ,

Altschuler, S. M., Bao, X., Bieger, D., Hopkins, D. A., and Miselis, R. R. (1989). Viscerotopic representation of the upper alimentary tract in the rat: Sensory ganglia and nuclei of the solitary and spinal trigeminal tracts. *J. Comp. Neurol.* **283**, 248–268.

Amaral, D. G., and Witter, M. P. (1995). Hippocampal formation. In G. Paxinos (Ed.), The Rat Nervous System, 2nd ed., Academic Press, San Diego, pp. 443–493..

Armstrong, W. E. (1995). Hypothalamic supraoptic and paraventricular nuclei. In G. Paxinos (Ed.), The Rat Nervous System, 2nd ed., Academic Press, San Diego, pp. 377–390.

Aston-Jones, G., Shipley, M. T., and Grzanna, R. (1995). The locus coeruleus, A5 and A7 noradrenergic cell groups. In G. Paxinos (Ed.), The Rat Nervous System, 2nd ed., Academic Press, San Diego, pp. 183–212.

Beitz, A. J. (1995). Periaqueductal Gray. In G. Paxinos (Ed.), The Rat Nervous System, 2nd ed., Academic Press, San Diego, pp. 173–182.

Berman, A. L. (1968). The Brainstem of the Cat: A Cytoarchitectonic Atlas with Stereotaxic Coordinates. University of Wisconsin Press, Madison.

Buttner-Ennever, J. A., Cohen, G., Pause, M., and Fries, W. (1988). Raphe nucleus of the pons containing omnipause neurons of the oculomotor system in the monkey, and its homologue in man. *J. Comp. Neurol.* **267**, 307–321.

Carrive, P. (1993). The periaqueductal gray and defensive behavior functional representation and neuronal organization. *Behav. Brain Res.* **58**, 27–47.

Carrive, P., and Paxinos, G. (1994). The supraoculomotor cap: A region revealed by NADPH diaphorase histochemistry. *NeuroReport* **5**, 2257–2260.

Cox, M., and Halliday, G. M. (1993). Parvalbumin as an anatomical marker for discrete subregions of the ambiguous complex in the rat. *Neuroscience Letters*, **160**, 101–105.

De Olmos, J., Hardy, H., and Heimer, L. (1978). The afferent connections of the main and the accessory olfactory bulb formation in the rat: An experimental HRP study. *J. Comp. Neurol.* **181**, 213–244.

Ellenberger, H. H., Feldman, J. L., and Zhan, W.-Z. (1990). Subnuclear organization of the lateral tegmental field in the rat. II: Catecholamine neurons and ventral respiratory group. *J. Comp Neurol.* **294**, 212–222.

Elmquist, J. K., Scammell, T. E., Jacobson, C. D., and Saper, C. B. (1996). Distribution of Fos-like immunoreactivity in the rat brain following intravenous lipopolysaccharide administration. *J. Comp. Neurol.* **371**, 1–19.

Fallon, J. H., and Loughlin, S. E. (1995). Substantia nigra. In G. Paxinos (Ed.), The Rat Nervous System, Academic Press, San Diego, pp. 215–237.

Faye-Lund, H., and Osen, K. K. (1985). Anatomy of the inferior colliculus in rat. *Anat. Embryol.* **171**, 1–20.

Franklin, K., and Paxinos, G. (1996). The Mouse Brain in Stereotaxic Coordinates. Academic Press, San Diego.

Fulwiler, C. E., and Saper, C. B. (1984). Subnuclear organization of the efferent connections of the parabrachial nucleus in the rat. *Brain Res. Rev.* **7**, 229–259.

Giolli, R. A., Blanks, R. H. I., Torigoe, Y., and Williams, D. D. (1985). Projections of medial terminal accessory optic nucleus, ventral tegmental nuclei, and substantia nigra of rabbit and rat as studied by retrograde axonal transport of horseradish peroxidase. *J. Comp. Neurol.* **232**(1), 99–116.

Grove, E. A. (1988). Efferent connections of the substantia innominata in the rat. *J. Comp. Neurol.* **277**,

347–364.
Halliday, G., Harding, A., and Paxinos, G. (1995). Serotonin and tachykinin systems. In G. Paxinos (Ed.), The Rat Nervous System, 2nd ed., Academic Press, San Diego, pp. 929–974.
Heimer, L., Zahm, D. S., Churchill, L., Kalivas, P., and Wohltmann C. (1991). Specificity in the projection patterns of accumbal core and shell in the rat. *Neuroscience* **41**, 89–125.
Heimer, L., Zahm, D. S., and Alheid, G. F. (1995). Basal ganglia. In G. Paxinos (Ed.), The Rat Nervous System, 2nd ed., Academic Press, San Diego, pp. 579–628.
Herbert, H., Moga, M., and Saper, C. (1990). Connections of the parabrachial nucleus with the nucleus of the solitary tract and the medullary reticular formation in the rat. *J. Comp. Neurol.* **293**, 540–580.
Hökfelt, T., Martensson, R., Bjorklund, A., Kleinau, S., and Goldstein, M. (1984). Distributional maps of tyrosine-hydroxylase-immunoreactive neurons in the rat brain. In A. Bjorklund and T. Hökfelt (Eds.), Handbook of Chemical Neuroanatomy, Vol. 2, Part 1. Elsevier, Amsterdam.
Jakab, R. L., and Leranth, C. (1995). Septum. In G. Paxinos (Ed.), The Rat Nervous System, 2nd ed., Academic Press, San Diego, pp. 405–442.
Jones, B. E. (1995). Reticular formation: Cytoarchitecture, transmitters, and projections. In G. Paxinos (Ed.), The Rat Nervous System, 2nd ed., Academic Press, San Diego, pp. 155–171.
Kanjhan, R., Lipski, J., Kruszewska, B., and Rong, W. (1995). A comparative study of pre-sympathetic and Bötzinger neurons in the rostral ventrolateral medulla (RVLM) of the rat. *Brain Research* **699**, 19–32.
Koelle, G. G., and Friedenwald, J. S. (1949). A histochemical method for localizing cholinesterase activity. *Proc. Soc. Exp. Biol. Med.* **70**, 617–622.
Konig, J. F. R., and Klippel, R. A. (1963). The Rat Brain: A Stereotaxic Atlas of the Forebrain and Lower Parts of the Brain Stem. Williams and Wilkins, Baltimore.
Kruger, L., Saporta, S., and Swanson, L. W. (1995). Photographic Atlas of the Rat Brain, Cambridge University Press, Cambridge.
Larsen, P.J. (1992). Distribution of substance P-immunoreactive elements in the preoptic area and the hypothalamus of the rat. *J. Comp. Neurol* **316**, 287–313.
LeDoux, J. E., Ruggiero, D. A., and Reis, D. J. (1985). Projections to the subcortical forebrain from anatomically defined regions of the medial geniculate body in the rat. *J. Comp. Neurol.* **242**, 182–213.
Lewis, P. R. (1961). The effect of varying the conditions in the Koelle method. *Biblthеca Anat. Vol. 2*, Karger, Basel, 11–20.
Magoul, R., Ciofi, P. and Tramu, G. (1994). Visualization of an efferent projection route of the hypothalamic rat arcuate nucleus through the stria terminalis after labeling with carbocyanine dye (DiI) or proopiomelanocortin-immunohistochemistry. *Neuroscience Letters* **172**,134–138.
Mai, J. K., Assheuer, J., and Paxinos, G. (in press).Atlas of the Human Brain. Academic Press, San Diego.
Malmierca, M. S., Rees, A., Le Beau, F. E., and Bjaalie, J. G. (1995). Laminar organization of frequency-defined local axons within and between the inferior colliculi of the guinea pig. *J. Comp. Neuro.* **357**(1), 124–44.
Marfurt, C., and Rajchert, D. M. (1991). Trigeminal primary afferent projections to “Non-Trigeminal” areas of the rat central nervous system. *J. Comp. Neurol.* **303**, 489–511.
McRitchie, D. A. (1992). Cytoarchitecture and chemical neuroanatomy of the nucleus of the solitary tract: Comparative and experimental studies in the human and the rat. Unpublished Ph.D. thesis, Univ. of New South Wales.
McRitchie, D. A., Hardman, C. D. and Halliday, G. M. (1996). Cytoarchitectural distribution of calcium binding proteins in midbrain dopaminergic regions of rats and humans. *J. Comp. Neurol.* **364**, 121–150.
Molander, C., and Grant, G. (1995). Spinal cord cytoarchitecture. In G. Paxinos (Ed.), The Rat Nervous System. Academic Press, San Diego.
Molander, C., and Gunnar, G. (1995). Spinal cord cytoarchitecture. In G. Paxinos (Ed.), The Rat Nervous System, 2nd ed., Academic Press, San Diego, pp. 39–44.
Morin, L. P., and Blanchard, J. (1995). Organization of the hamster intergeniculate leaflet: NPY and ENK projections to the suprachiasmatic nucleus, intergeniculate leaflet and posterior limitans nucleus. *Visual*

Neuroscience **12**, 57–67.
Neafsey, E. J., Bold, E. L., Haas, G., Hurley-Gius, K. M., Quirk, G., Sievert, C. F., and Terreberry, R. R. (1986). The organization of the rat motor cortex: A microstimulation mapping study. *Brain Research Rev.* **11**, 77–96.
Norgren, R. (1995). Gustatory system. In G. Paxinos (Ed.), The Rat Nervous System, 2nd ed., Academic Press, San Diego, pp. 751–771.
Oldfield, B. J., and McKinley, M. (1995). Circumventricular organs. In G. Paxinos (Ed.), The Rat Nervous System, 2nd ed., Academic Press, San Diego, pp.391–403.
Paxinos, G. (Ed.) (1995). The Rat Nervous System, 2nd. ed., Academic Press, San Diego.
Paxinos, G., and Huang X.-F. (1995). Atlas of the Human Brainstem. Academic Press, San Diego.
Paxinos, G., and Watson, C. (1996). The Rat Brain in Stereotaxic Coordinates, Compact 3rd Edition CD-Rom. Academic Press, San Diego.
Paxinos, G., and Watson, C. (1982) The Rat Brain in Stereotaxic Coordinates. Academic Press, San Diego.
Paxinos, G., and Watson, C. (1986). The Rat Brain in Stereotaxic Coordinates, 2nd ed. Academic Press, San Diego.
Paxinos, G. *et al*., (in press [a]) *The rat forebrain: A comprehensive atlas based on seven chemical markers*, Academic Press, San Diego.
Paxinos, G. *et al*. (in press [b]). The Rat Brainstem. A Comprehensive Atlas Based on Seven Chemical Markers, Academic Press, San Diego.
Paxinos, G., Ashwell, K.W., and Tork, I. (1994). Atlas of the Developing Rat Nervous System, Second edition, Academic Press, San Diego.
Paxinos, G., Tork, I., Halliday, G., and Mehler, W. R. (1990). Human homologs to brainstem nuclei identified in other animals as revealed by acetylcholinesterase. In G. Paxinos (Ed.), The Human Nervous System, Academic Press, San Diego, pp.149–202.
Paxinos, G., Watson, C., Pennisi, M., and Topple, A. (1985). Bregma, lambda and the interaural midpoint in stereotaxic surgery with rats of different sex, strain and weight. *J. Neurosci. Meth*. **13**, 139–143.
Price, J. L. (1995). Thalamus. In G. Paxinos (Ed.), The Rat Nervous System, 2nd ed., Academic Press, San Diego, pp. 629-648.
Ray, J. P. and Price, J. L. (1992). The organization of the thalamocortical connections of the mediodorsal thalamic nucleus in the rat, related to the ventral forebrain-prefrontal cortex topography. *J. Comp. Neurol.* **323**, 167–197.
Ruigrok, T. J. H., and Cella F. (1995). Precerebellar nuclei and red nucleus. In G. Paxinos (Ed.), The Rat Nervous System, 2nd ed., Academic Press, San Diego, pp. 277-308.
Saper, C. B. (1995). Brain stem and cerebellum, central autonomic system: In G. Paxinos (Ed.), The Rat Nervous System, 2nd ed., Academic Press, San Diego, pp. 107–135.
Sefton, A. J., and Dreher, B. (1995). Visual system. In G. Paxinos (Ed.), The Rat Nervous System, 2nd ed., Academic Press, San Diego, pp. 833–898.

Sherin, J. E., Shiromani, P. J., McCarley, R. W., and Saper, C. B. (1996). Activation of ventrolateral preoptic neurons during sleep. *Science* **271**, 216–219.

Shipley, M. T., and McLean, J. H., and Ennis, M. (1995). Olfactory system. In G. Paxinos (Ed.), The Rat Nervous System, 2nd ed., Academic Press, San Diego, pp. 899–926.

Simerly, R. B. (1995). Anatomical substrates of hypothalamic integration. In G. Paxinos (Ed.), The Rat Nervous System, 2nd ed., Academic Press, San Diego, pp. 353–376.

Simerly, R. B., Swanson, L. W., and Gorski, R. A. (1984). Demonstration of a sexual dimorphism in the distribution of serotonin-immunoreactive fibers in the medial preoptic nucleus of the rat. *J. Comp. Neurol.* **225**, 151–139.

Slotnick, B. M., and Brown, D. L. (1980). Variability in the stereotaxic position of cerebral points in the albino rat. *Brain Res. Bull.* **5**, 135–139.

Swanson, L. W. (1992). Brain Maps: Structure of the Rat Brain. Elsevier, Amsterdam.

Tracey, D. J., and Waite, P. M. E. (1995). Somatosensory system. In G. Paxinos (Ed.), The Rat Nervous System, 2nd ed., Academic Press, San Diego, pp. 689–704.

Travers, J. B. (1995). Oromotor nuclei. In G. Paxinos (Ed.), The Rat Nervous System, 2nd ed., Academic Press, San Diego, pp. 239–250.

Van Groen, T., and Wyss, J. M. (1992). Connections of the retrosplenial dysgranular cortex in the rat. *J. Comp. Neurol.* **315**, 200–216.

Voogd, J. (1995). Cerebellum. In G. Paxinos (Ed.), The Rat Nervous System, 2nd ed., Academic Press, San Diego, pp. 309–350.

Waite, P. M. E., and Tracey, D. J. (1995). Trigeminal sensory system. In G. Paxinos (Ed.), The Rat Nervous System, 2nd ed., Academic Press, San Diego, pp. 705–724.

Wang, P. Y., and Zhang, F. C. (1995). Outlines and Atlas of Learning Rat Brain Slides. Westnorth University Press, China.

Webster, W. R. (1995). Auditory system. In G. Paxinos (Ed.), The Rat Nervous System, 2nd ed., Academic Press, San Diego, pp. 797–831.

Whishaw, I. Q., Cioe, J. D. D., Previsich, N., and Kolb, B. (1977). The variability of the interaural line vs the stability of bregma in rat stereotaxic surgery. *Physiol. Behav.* **19**, 719–722.

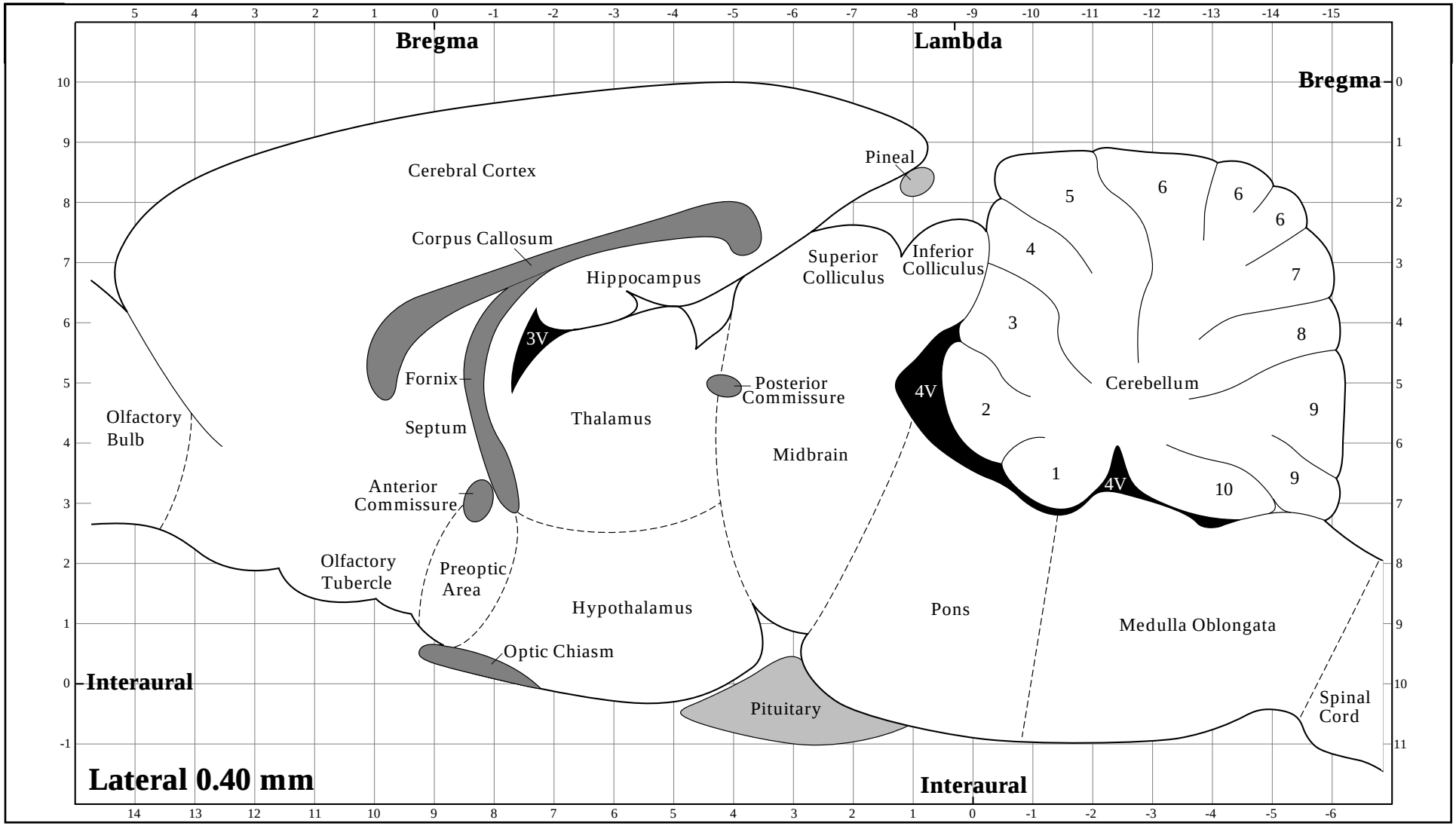
Whitehead, M. C. (1990). Sibdivisions and neruon types of the nucleus of the solitary tract in the hamster. *J. Comp. Neurol.* **310**, 554–574.

Yasui, Y., Saper, C., and Cechetto, D. (1989). Calcitonin gene-related peptide immunoreactivity in the visceral sensory cortex, thalamus, and related pathways in the rat. *J. Comp. Neurol.* **290**, 487–501.

Zaborszky, L., Alheid, G. F., Beinfeld, M. C., Eidens, L. E., Heimer, L., and Palkovits, M. (1985). Cholecystokinin innervation of the ventral striatum: A morphological and radioimmunological study. *Neurosci.* **14**, 427–453.

Zilles, K. (1985). The Cortex of the Rat: A Stereotaxic Atlas. Springer-Verlag, Berlin.

Zilles, K., and Wree, A. (1995). Cortex: areal and laminar structure. In G. Paxinos (Ed.), The Rat Nervous System, 2nd ed., Academic Press, San Diego, pp. 649–685.



Sagittal section of the rat brain. A drawing of a section of the rat brain cut in a sagittal plane 0.4 mm lateral to the midline. The drawing was made from a photograph of a Nissl-stained sagittal section (Plate 78 in Paxinos and Watson, 1986). Almost all major regions of the brain can be seen in this section, so that it can be used as a guide to the position of the coronal sections of the brain (Figs. 1–76). A miniature version of this section is shown at the top left of Figs. 1–76 (the section plan) to mark the position of each coronal section. The only major regions of the brain not pictured here are the anterior part of the olfactory bulb, which has been cut off at the left of the section, and the subcortical nuclei (caudatoputamen, globus pallidus, and the amygdala), which are located about 3–5 mm lateral to this sagittal plane. Parts of the ventricular system of the brain can be seen in this section (represented in solid black). Note that the pituitary gland can be seen ventral to the hypothalamus and the pineal gland can be seen dorsal to the superior colliculus. It should be noted that the boundaries between some of the brain regions pictured here are approximations, since the arbitrary classification of cell groups as belonging to one area or another does not always result in sharp lines of regional demarcation. The position of skull landmarks (bregma, lambda, and the interaural line) are shown in this figure. The top grid line indicates anteroposterior locations in relation to a coronal plane passing through bregma. The bottom grid line shows anteroposterior locations in relation to a coronal plane passing through the interaural line. The left vertical grid line shows dorsoventral locations in relation to a horizontal plane passing through bregma. The right vertical grid shows dorsoventral positions in relation to a horizontal plane passing through the interaural line.